

# Time-resolved Langmuir Probing of a New Lanthanum Hexaboride (LaB<sub>6</sub>) Hollow Cathode

IEPC-2011-245

*Presented at the 32nd International Electric Propulsion Conference,  
Wiesbaden • Germany  
September 11 – 15, 2011*

Kimberly R. Trent<sup>1</sup> and Michael S. McDonald<sup>2</sup>  
*Plasmadynamics and Electric Propulsion Laboratory, University of Michigan, Ann Arbor, MI 48104, USA*

Robert B. Lobbia<sup>3</sup>  
*Air Force Research Laboratory, Edwards, CA 93524, USA*

and

Alec D. Gallimore<sup>4</sup>  
*Plasmadynamics and Electric Propulsion Laboratory, University of Michigan, Ann Arbor, MI, 48104, USA*

**Abstract:** A new laboratory model lanthanum hexaboride (LaB<sub>6</sub>) hollow cathode sized for a 20 A HET discharge has been developed. The cathode design is based on previous high-current LaB<sub>6</sub> cathodes. The cathode's heating element, which is used to bring the insert to thermionic emission temperatures, is usually the most likely to break down. In this new LaB<sub>6</sub> cathode, the heater has been redesigned to address various fail mechanisms such as the fusion of the heating element to other critical elements of the cathode, and the high-cost of replacing this component of the cathode. This relatively low-cost, and robust cathode was designed for use in experiments to aid in the contemporary modeling of electron dynamics in Hall-effect Thrusters (HETs), and for use in experiments to aid in the development of methods for electron energy distribution function (EEDF) control in HETs. In preparation for these experiments, this cathode was run in triode mode with an annular anode, and stable operation was achieved for various operating conditions. Various plasma parameters were calculated from Langmuir probe (LP) data at a point downstream in the plasma plume. The EEDF was also determined from this data and is best described by a Maxwellian distribution function with a velocity shift.

## Nomenclature

$A_p$	=	Langmuir probe tip area, m <sup>2</sup>
$\Delta v$	=	velocity shift that corresponds to the potential shift used as a fit parameter in $g_{M+v}(V)$ , m/s
$\Delta V$	=	potential shift used in $g_{M+v}(V)$ to fit the distribution to the measured EEDF, V
$g_e(V)$	=	measured EEDF, 1/(m <sup>3</sup> ·eV)
$g_{M+v}(V)$	=	Maxwellian with velocity shift distribution function, 1/(m <sup>3</sup> ·eV)
$I_{anode}$	=	anode current, A
$I_e$	=	Langmuir probe collected electron current, A

<sup>1</sup> Doctoral Pre-candidate, Applied Physics Program, [kimtrent@umich.edu](mailto:kimtrent@umich.edu).

<sup>2</sup> Doctoral Candidate, Applied Physics Program, [mrmcdon@umich.edu](mailto:mrmcdon@umich.edu).

<sup>3</sup> Electric Propulsion Engineer, Spacecraft Branch RZSS, [robert.lobbia.ctr@edwards.af.mil](mailto:robert.lobbia.ctr@edwards.af.mil).

<sup>4</sup> Arthur F. Thurnau Professor, Aerospace Engineering, Plasmadynamics and Electric Propulsion Laboratory Director, [rasta@umich.edu](mailto:rasta@umich.edu).

$I_{keeper}$	=	keeper current, A
$\dot{m}$	=	argon gas flow rate
$m_e$	=	electron mass, kg
$m_i$	=	argon ion mass, kg
$N_e$	=	electron number density, m <sup>-3</sup>
$P_b$	=	chamber base pressure, torr
$T_{e,EEDF}$	=	electron temperature calculated from the measured EEDF, eV
$T_{e,fit}$	=	electron temperature used in $g_{M+\nu}(V)$ to fit the distribution to the measured EEDF, eV
$T_{e,potential}$	=	electron temperature calculated from the potential method, eV
$T_{e,slope}$	=	electron temperature calculated from the slope method, eV
$T_r$	=	run time, hours
$V_{anode}$	=	anode voltage, V
$V_b$	=	Langmuir probe bias voltage, V
$V_{C-G}$	=	cathode-to-ground voltage, V
$V_f$	=	floating potential, V
$V_{keeper}$	=	keeper voltage, V
$V_p$	=	plasma potential, V

## I. Introduction

THE hollow cathode was first discussed by Paschen in 1916. His setup featured a thin rectangular hollow cathode made of a sheet of aluminum and a cylindrical anode, and was used as the excitation source to analyze the spectral lines of helium. The hollow cathodes used today have a wide variety of applications, and their designs are all versions of Paschen's initial cathode yet modified for the particular implementation.<sup>1</sup> Over the years, the applications of hollow cathodes have included use as the excitation source in analytical spectroscopy, as done by Paschen, the ion source for industrial thin film application, the electron source in scanning electron microscopes, and the electron source for plasma volume neutralization in electric thrusters. Lanthanum hexaboride (LaB<sub>6</sub>) was first investigated for use as an electron emitter by Lafferty in the late 1940s.<sup>2</sup> The Russians have used LaB<sub>6</sub> hollow cathodes in Hall thrusters from the first flight of a stationary plasma thruster (SPT) in 1972.<sup>3</sup> In the United States, barium-oxide impregnated (BaO-W) dispenser hollow cathodes were used initially, starting in the 1960s.<sup>4</sup> These cathodes make use of a tungsten-based insert that is gridded with holes, filled with a barium, calcium oxide, and alumina mix. When heated to temperatures around 1000°C, this mixture dispenses electrons from these openings in the tungsten. LaB<sub>6</sub> is made by press-sintering lanthanum hexaboride powder into a solid, polycrystalline (i.e., multiple crystal orientation) form.<sup>5</sup>

Lanthanum hexaboride requires a higher operating temperature than BaO-W, and the US did not begin to consider LaB<sub>6</sub> for hollow cathodes, for space-application, until the 1970s. Compact high current cathodes became of interest at this time for future applications that would require high current densities such as high-power electric thrusters that are able to deliver a higher thrust. Experimental data for BaO-W and LaB<sub>6</sub> calculations using Richardson and evaporation coefficients ascertained by Lafferty show that BaO-W has a maximum emission current density of 12 A/cm<sup>2</sup> at an operation temperature of ~1100°C, whereas LaB<sub>6</sub> can provide 40 A/cm<sup>2</sup> of current density at a temperature of 1800°C.<sup>6</sup> For comparison, LaB<sub>6</sub> provides ~12 A/cm<sup>2</sup> at around 1510°C.<sup>7</sup> In addition to their high current density, LaB<sub>6</sub> has a longer calculated insert lifetime than a BaO-W insert by almost an order of magnitude for discharge currents from 10 A to 60 A. These calculations take into account the evaporate rate of these materials which is lower for LaB<sub>6</sub>, despite its substantially higher operating temperature, up to an emission current density of 15 A/cm<sup>2</sup>. This slightly lower evaporation rate and the fact that there is more bulk emitting material in LaB<sub>6</sub>, than in the impregnated holes of the tungsten matrix in BaO-W dispenser material, are what account for the longer LaB<sub>6</sub> lifetime. These calculations did not take into account impurity build-up, which reduces lifetime and re-deposition of some insert material after evaporation, which increases lifetime.<sup>5</sup>

Another advantage of LaB<sub>6</sub> is that special conditioning and storage procedures do not have to be followed, because this material is not susceptible to contamination from oxygen and water vapor, which can raise the work function of BaO-W, decreases its life, and often times cease emission from the material altogether rendering the dispenser cathode completely useless. The reason for this is that in BaO-W, a chemical reaction needs to take place in the barium, calcium oxide, and alumina mixture at the 1000°C operation temperatures in order for a barium-oxide dipole to form to reduce the work function of the surface to ~2 eV. This is what allows this material to be an abundant source of electrons. In comparison, with LaB<sub>6</sub>, the formation of a low work function on the material's surface does not involve a chemical reaction. The lanthanum hexaboride itself is the electron emitter and has a work

function of  $\sim 2.7$  eV at a temperature of  $1650^\circ\text{C}$ . Therefore, a  $\text{LaB}_6$  insert's emission capability is relatively unaffected by impurities that can hinder the chemical reactions necessary in BaO-W cathodes.<sup>8</sup>

In a hollow cathode, once the insert material reaches emission temperatures, applying a high voltage to the keeper will accelerate the electrons. This draws the electrons out of the insert region and starts the plasma discharge. Once the discharge is established, the keeper voltage will decrease and level out to a value that will maintain the insert temperature, allowing the discharge to be self-sustaining. This is because the voltage drop between the keeper and insert that pulls electrons from the cathode also causes ions to flow into the cathode. These ions accelerate through the sheath and collide with the insert. This heats the insert causing more electrons to be emitted, which collide with the flowing gas causing more ions to be formed. If the current decreases, then the voltage drop, and hence the keeper discharge voltage, increases to maintain the insert temperature. Therefore, once the discharge is established, the heater can be turned down. However, this self-heating mechanism is also dependent on the current. If the discharge current is too low, then the discharge voltage will not be able to maintain the insert temperature, and the plasma will die out.

## II. Motivation

The  $\text{LaB}_6$  cathode presented in this paper has been developed to use as the plasma source for initial experiments to study electron dynamics in Hall-effect thrusters (HETs). Since the cathode is the main source of electrons for the thruster, and can be operated with a relatively smaller scale production than the thruster, it serves as an ideal platform for testing the electron dynamic experimental procedures and diagnostic tools that will be used for various projects. Two of these projects, which are currently being carried out in the lab, involve the tracking of electrons in the HET plume for modeling purposes, and the control of the electron energy distribution function (EEDF) to improve thruster efficiency. These will be described in more detail below.

### A. Electron Dynamics Modeling

Treatment of the cathode and of electron transport in general is a grey area in many HET models. In some, such as the quasi-1D HPHall-2,<sup>9</sup> a “virtual cathode” sources electrons from a magnetic field line downstream of the exit plane, with anomalous electron transport parameters chosen to match established experimental performance parameters such as thrust and discharge current as closely as possible. In other cases, such as the fully 3D electron trajectory simulator MCHall,<sup>10</sup> electrons are sourced at the correct physical location of the cathode but from time-averaged experimental measurements of cathode plume plasma potentials and with an assumed Maxwellian distribution about time-averaged experimental electron temperatures. However, attempts at physically accurate models are hampered by the lack of time-resolved measurements in the cathode region, and a poor understanding of how electrons from the cathode couple into the main thruster discharge.

To help bridge this gap, a series of high-speed diagnostics will be performed using this cathode in triode mode to simulate the near-cathode region of a full Hall thruster discharge. This will serve as a first step in developing a full time-resolved dataset spanning the Hall thruster cathode-to-discharge channel exit plane region.

### B. Electron Energy Distribution Function (EEDF) Control

One approach to increasing HET efficiency is the predictive control of the EEDF. HET efficiency depends on its ability to ionize and accelerate neutral propellant to produce thrust. The ability to control the EEDF would allow electrons with energies that contribute to ionization to be increased, and those involved in transient processes (or those that do not have enough energy to ionize) to be reduced. What makes predictive EEDF control a challenge is the complex electromagnetic interactions that take place in the HET between the thruster's magnetic field, electric field and ionized propellant (plasma), which lead to the turbulent nature of these plasmas.

As an initial step in tackling this problem, this hollow cathode will be run in triode mode and various EEDF control methods will be evaluated by taking spatial maps of time-resolved Langmuir probe data to obtain EEDF profiles, which will be compared to determine the effect of these methods on the plasma. The purpose of these experiments is to demonstrate various methods for EEDF control with one component of the HET system. From these results we will be able to make predictions about how the rest of the HET system may respond before actually conducting this testing. Therefore, results from these experiments will allow us to develop possible predictive control methods to increase efficiency in the full HET system.

If HET efficiency can be further increased for operation in the low-power range, this will enable more complex and extensive missions. Proposed science missions that could be enabled with higher performance propulsion systems include robotic missions to the Moon, Mars, and near-Earth asteroids to perform round trip sample-returns,

to search for and prepare resources, to set up sites in anticipation of future landings, and to demonstrate new technology in preparation for even more challenging and longer-range robotic missions.

### III. Cathode Development

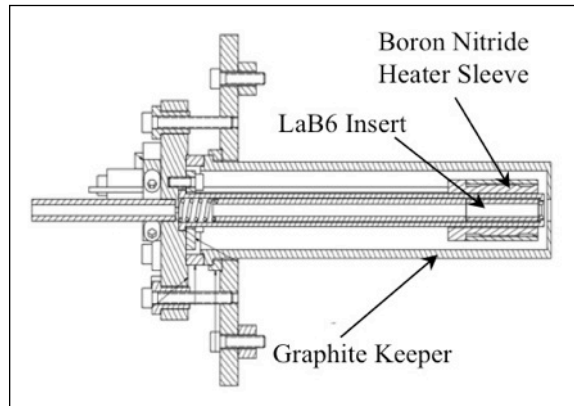
The hollow cathode designed for these tests is based on high-current LaB<sub>6</sub> cathodes<sup>8</sup> used in the H6, a 6-kW laboratory model Hall thruster developed at the Air Force Research Laboratory (AFRL) with the Jet Propulsion Laboratory (JPL) and the Plasmadynamics and Electric Propulsion Laboratory (PEPL). This thruster is described elsewhere.<sup>7</sup> LaB<sub>6</sub> cathode inserts have an area that is too large for direct heating because the resistance of the material is too low, so the insert must be heated indirectly to bring it to thermionic emission temperatures in the range of 1500-2000 K.<sup>6</sup> Unfortunately, the most failure-prone component of LaB<sub>6</sub> cathodes is generally the heating element. The gradual but inevitable failure of the heating element and occasional irreversible fusion of the heating element to other critical elements of the cathodes previously used in the 6-kW Hall thruster motivated the construction of a low-cost, robust cathode with an alternative heater and a more graceful failure mode.

#### A. Overall Cathode Design

This cathode features a graphite insert retaining tube and a graphite keeper with an outer diameter of less than 25.4-mm. These parts were made out of graphite because this material is easily machinable, it has a high melting point, and unlike refractory metals such as tungsten and molybdenum, it is not susceptible to boron diffusion from



a)



b)

**Figure 1. Lab-built Hollow Cathode.**

a) Operation of the LaB<sub>6</sub> cathode without an anode

b) Cutaway cross section (right) of the cathode showing the boron nitride ceramic sleeve used as a heat spreader for the heating filament.

the LaB<sub>6</sub> insert or the boron nitride heater sleeve. Boron diffusion leads to the embrittlement of these materials, which jeopardizes the structural integrity of the cathode.<sup>2</sup> Similar to previous cathodes, the LaB<sub>6</sub> insert has a 6.35-mm outer diameter, a thickness of 1.27-mm, and is 25.4-mm in length. Since this length is approximately one-fifth the length of the

graphite cathode tube, the insert is held against the orifice by an insert spacer and a 12.7-mm tungsten spring (Fig. 1). The insert's 3-cm<sup>2</sup> interior surface area is the insert's emission area. According to the Richardson-Dushman equation, the LaB<sub>6</sub> insert material can emit 20-A/cm<sup>2</sup> at a temperature of 1700°C.<sup>11</sup> Therefore, this cathode has an upper emission current of around 60 A. For these initial tests, the keeper and anode currents were limited to a maximum of 9A.

#### B. Heater Design

The new heater design is composed of an HP grade boron nitride (BN) ceramic heat spreader and a filament with a diameter of 0.254-mm (Fig. 2). The heat spreader is electrically isolating but very thermally conductive. It completely encloses the heater wire to reduce the possibility of a heater-keeper short. Instead of a helical wire path in the ceramic heat spreader, an axial pattern is used to make the machining of the BN sleeve easier (Fig. 2c).

Two alumina tubes provide an outbound and return path for the heater wire, eliminating the need to spot-weld the wire to the cathode tube itself, and permitting easy mechanical attachment, assembly, and disassembly (Appendix A). The alumina tubes guide the wires up to the gas adapter flange. Two thick tungsten wires are attached to the heater and cathode electrical connections on the gas adapter flange and are fed into the tubes from the gas adapter flange end. To form a solid electrical connection between these wires and the heater filament leads, the tubes are friction fit with thin pieces of tungsten wire.

The ensuing subsections will go over various aspects of the design optimization process, which led to the current design. In this optimization process, we had to consider materials' compatibility, heat loss mechanisms, and the reliability and robustness of the design.



**Figure 2. Photographs of the Lab-built Hollow Cathode.**

*a) The full hollow cathode assembly.*

*b) The cathode with keeper electrode and radiation sleeve removed.*

*c) A close up of the boron nitride heater inner and outer sleeves, the inlaid heater filament wire, and the alumina heater wire lead tubes.*

### 1. Design Adjustments to Reduce Heat Loss

To quantify how the power from the heater was being deposited in the cathode, and whether the design and heat shielding were thermally efficient, several thermocouple tests were carried out to determine how hot the cathode was getting. A thermocouple was placed on the front face of the keeper and another on the orifice, which touches the insert. In the test results we looked to see whether the orifice, and hence the insert, was reaching the thermionic emission temperature for  $\text{LaB}_6$ ,  $\sim 1650^\circ\text{C}$ , what temperature the keeper was reaching, and the amount of time it took for the insert's temperature to level off after the current to the heater is increased.

We found that the cathode orifice reached  $1000^\circ\text{C}$  and was therefore still a ways off from the insert's thermionic emission temperatures. The keeper reached a little less than half this temperature. From this we concluded that the cathode was still able to light under these conditions because some of the electrons in the tail of the energy distribution would still be hot enough to escape the material. In addition, the insert itself may have been slightly hotter than the orifice. Still, the average temperature of the insert was probably significantly lower than  $1650^\circ\text{C}$ . This may, for the most part, account for the higher keeper ignition voltages needed for the earlier prototype of this cathode and the fact that it was still difficult to light this earlier version even with higher ignition voltages. To improve the heat transfer to the insert and to decrease the ability of the keeper to act as a conduction path for heat away from the insert, towards the gas adapter flange, we had a keeper with thinner walls machined, and added tantalum heat shielding along the entire length of the cathode (i.e., insert retaining) tube.

During these thermocouple tests, we noted that after a 2-A increase in current to the heater filament, the orifice would reach three quarters of its new equilibrium temperature in about 10 minutes. From this result, we were able to optimize our insert heating procedure.

### C. Cost Benefits of the New Design

The original heater design for these cathodes is an alumina-insulated tantalum-sheathed heater<sup>5</sup> that costs about \$800. It is prone to intermittent shorting after extended operation of a few tens to low hundreds of hours due to a gradual breakdown of the insulation material at  $\text{LaB}_6$  operating temperatures. This has been observed to be the main point of failure in the cathode in experiments

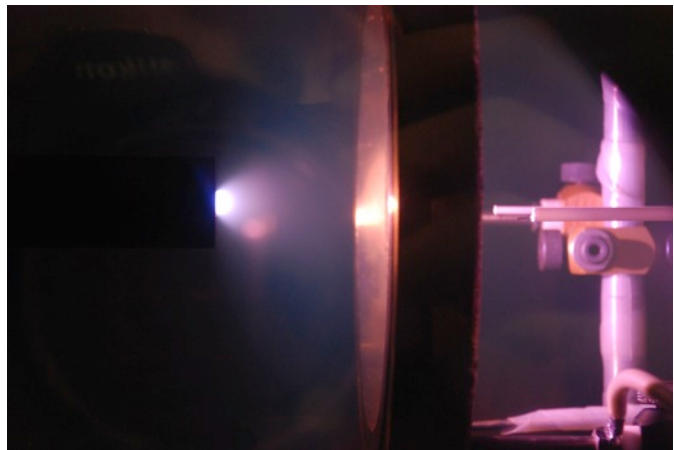


**Figure 3. Operation of Cathode in Triode Mode.**

*This figure shows the cathode plume in triode mode. The plasma fans out towards the edges of the anode and is noticeably brighter in this mode. The Langmuir probes and the anode's support structure are seen on the far right in this photo.*

with the H6 Hall thruster at the University of Michigan and Air Force Research Laboratory, with intermittent heater-keeper shorts also being an issue. It is worth noting that a third copy of the cathode with the original heater used at Jet Propulsion Laboratory is still in operation after approximately one thousand hours, indicating that some of the curtailed lifetime at AFRL and UM may be due to procedural differences in cathode operation between these institutions and JPL. The heater cost and its custom-order requirement prevent rapid turnaround in the event of heater failure. Additionally, cathode-keeper shorts were identified to be caused by axial creep of the original heater's helical winding, such that the tip had to be spot-welded to the cathode tube to prevent recurring shorts. The weld makes cathode disassembly for other purposes inordinately difficult, such as for replacement of an eroded orifice plate or a degraded LaB<sub>6</sub> insert.

In the event of a failure in the new heater design, the only new component required to fix the cathode is a length of refractory heater wire shaped into the necessary pattern to fit in the sleeves. For the total heater filament length of about 40 cm including the leads, this costs between \$5-35 depending on the wire material and diameter chosen for the design. The cost savings are about 95% of the original sheathed heater, and with care the filament can be shaped by hand, enabling in-house cathode disassembly and reassembly in a matter of hours (Appendix B). Once machined, the boron nitride sleeves do not need to be replaced.

A final note on the sleeve material: boron nitride has a chalk-like texture and is easily machineable with standard tooling. Competing thermally conductive but electrically insulating ceramics such as aluminum nitride (AlN) are machineable only by grinding, making the BN sleeves considerably more affordable to fabricate. Care must also be taken to only use pure BN (i.e., Saint-Gobain grade AX05). So-called high-purity grades, such as those typically used in Hall thruster discharge channels (i.e., Saint-Gobain grade HP), have binders that melt above 1300 K.

#### IV. Initial Characterization of Cathode Plume in Triode Mode

Triode mode operating points along with various time-resolved plasma properties for a single spatial location will be discussed in this section as a first look at the characteristics of this plasma source.

**Table 1. Cathode Operating Points.**

The table shows various operating points for the cathode in triode mode using an annular anode. In all the cases listed, the argon gas flow rate was 25 sccm, and the chamber base pressure without cathode gas flow was  $1 \times 10^{-7}$  torr.

Sustained Cathode Operating Points			
Case	1	2	3
$P_b$ (torr)	$5.9 \times 10^{-5}$	$2.3 \times 10^{-5}$	$3.4 \times 10^{-5}$
$V_{anode}$ (V)	20 V	37 V	15 V
$I_{anode}$ (A)	3.51 A	4.7 A	2.05 A
$V_{keeper}$ (V)	32 V	27.49 V	39.7 V
$I_{keeper}$ (A)	9 A	9 A	9 A
$V_{C-G}$ (V)	-2.5 V	-2.7 V	-2.3 V
$T_r$ (hours)	4 hours	2 hours	2 hours

#### A. Triode Mode Operating Points

The hollow cathode used in these experiments was run in triode configuration with an external annular anode, mimicking a conventional Hall thruster (but without anode flow), to permit operation in plume mode for extended periods (Fig. 3).

For the operating points shown in Table 1, a voltage was applied to the anode after the cathode settled into a relatively stable cathode-keeper operating mode. This was inferred by the settling of the cathode-to-ground voltage,  $V_{C-G}$ , to a narrow range. Therefore, the keeper also has a dominant role in these operating conditions. While the plasma stayed stable enough for taking

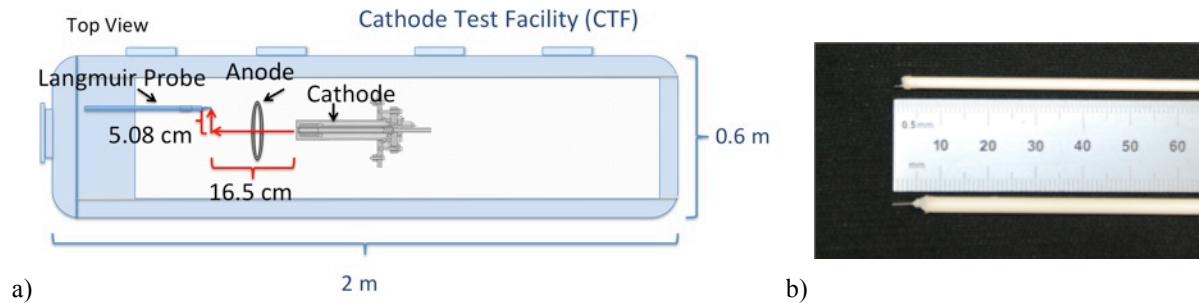


**Figure 4. Langmuir Probe Setup.**

- a) The cathode, anode and Langmuir probe (LP) orientation in the Cathode Test Facility (CTF)
- b) The upper LP, with a 0.127-mm diameter and 1.27-mm length, was used to obtain the LP trace.

data in these modes, operating points where the keeper is set to a lower voltage after the anode voltage is set were also established after these tests. In these modes, the keeper plays more of its usual, secondary role where it merely acts to “keep” the plasma.

## B. Time-resolved Measurements

A lab-built dual Langmuir probe system<sup>12</sup> was used to obtain measurements of electron density, electron temperature, plasma potential, and the EEDF. A sweep rate of 100 Hz along with a 1-MHz sampling rate were used. These measurements were carried out at the Plasmadynamics and Electric Propulsion Laboratory (PEPL) in the Cathode Test Facility (CTF). This cylindrical vacuum chamber is 2-m long and 0.6-m in diameter (Fig. 4a). The chamber obtains a base pressure of  $1 \times 10^{-7}$  torr. The Langmuir probe (LP) measurement was taken 5.08-cm from the centerline of the cathode’s exit plane, and 16.5-cm downstream (Fig. 4a). The LP used has a 0.127-mm probe tip diameter and a probe tip length of 1.27-mm (Fig. 4b). Figure 5 shows the time-resolved LP trace taken at the location shown in Fig. 4a. This trace was taken from one of the positive-sloping sides of the sine sweep waveform used to obtain the LP traces. While this measurement was being taken, the argon gas flow rate,  $\dot{m}$ , was 25 sccm,  $P_b = 5.9 \times 10^{-5}$  torr,  $V_{anode} = 32$  V,  $I_{anode} = 3$  A,  $V_{keeper} = 42$  V,  $I_{keeper} = 9$  A and  $V_{C-G} = -2.5$  V. The plasma properties calculated from this individual LP trace are a floating potential,  $V_f$ , of 20.88 V, a plasma potential,  $V_p$ , of 42.82 V, and an electron number density,  $N_e$ , of  $4.2 \times 10^{17} \text{ m}^{-3}$ . The electron temperature, when calculated as the inverse slope of the natural log of the electron current,  $T_{e,slope}$ , is 5.62 eV, and it is equal to 4.69 eV when calculated using

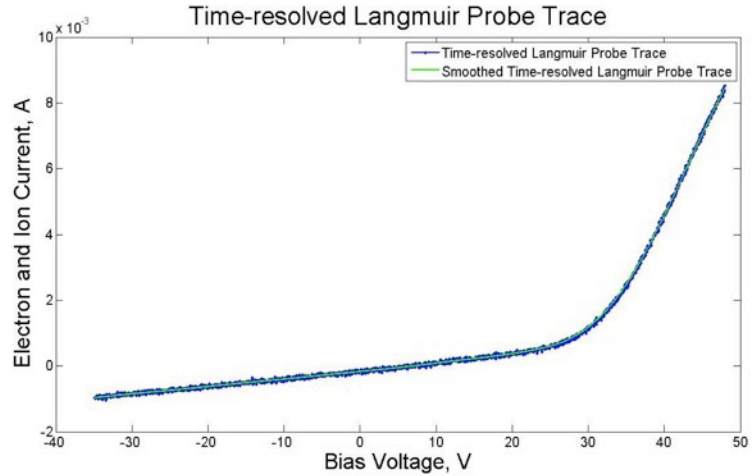


**Figure 5. Langmuir Probe Trace.**

The raw time-resolved LP trace taken from a positive-sloping side of the sine-wave bias-voltage waveform is shown in blue. The green line is the smoothed version of this trace, which was used to obtain the plasma parameters and EEDF.

$$T_{e,potential} = \frac{V_p - V_f}{\ln \left[ \sqrt{\frac{m_i}{2 \pi m_e}} \right]} \quad (1)$$

Both of these methods for calculating the electron temperature assume that the EEDF is a pure Maxwellian distribution.<sup>13</sup> Figure 6 shows the actual measured EEDF of the plasma at this location. This EEDF was calculated using Eq. (2)<sup>14</sup>, where the EEDF is derived using the second derivative of the I-V trace.

$$g_e(V) = \frac{2 m_e}{e^2 A_p} \sqrt{\frac{2 e}{m_e} \frac{d^2 I_e}{dV^2} \sqrt{V_s - V_b}} \quad (2)$$

The electron temperature,  $T_{e,EEDF}$ , calculated from integrating the actual EEDF, is 7.96 eV. This distribution most closely matches a Maxwellian with a velocity shift<sup>15</sup> as also shown in this figure. The equation for this distribution is

$$g_{M+v}(V) = \frac{2}{\sqrt{\pi}} N_e (T_{e,fit} \cdot \Delta V)^{-\frac{3}{2}} e^{-\frac{(V_s - V_b) + \Delta V}{T_{e,fit}}} \sinh \left\{ \frac{2[(V_s - V_b)(\Delta V)]^{1/2}}{T_{e,fit}} \right\} \sqrt{V_s - V_b} \quad (3)$$

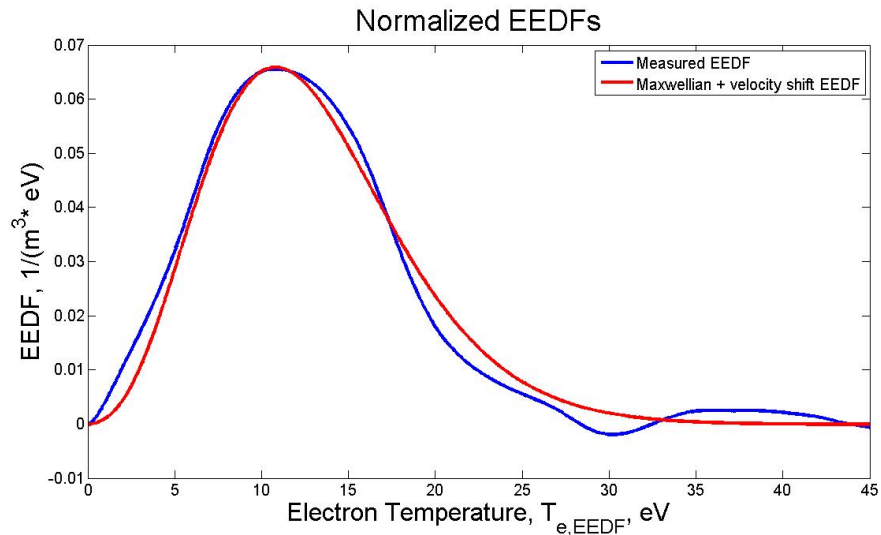


**Figure 6. Measured EEDF and Maxwellian with Velocity Shift EEDF Curve Fit.**

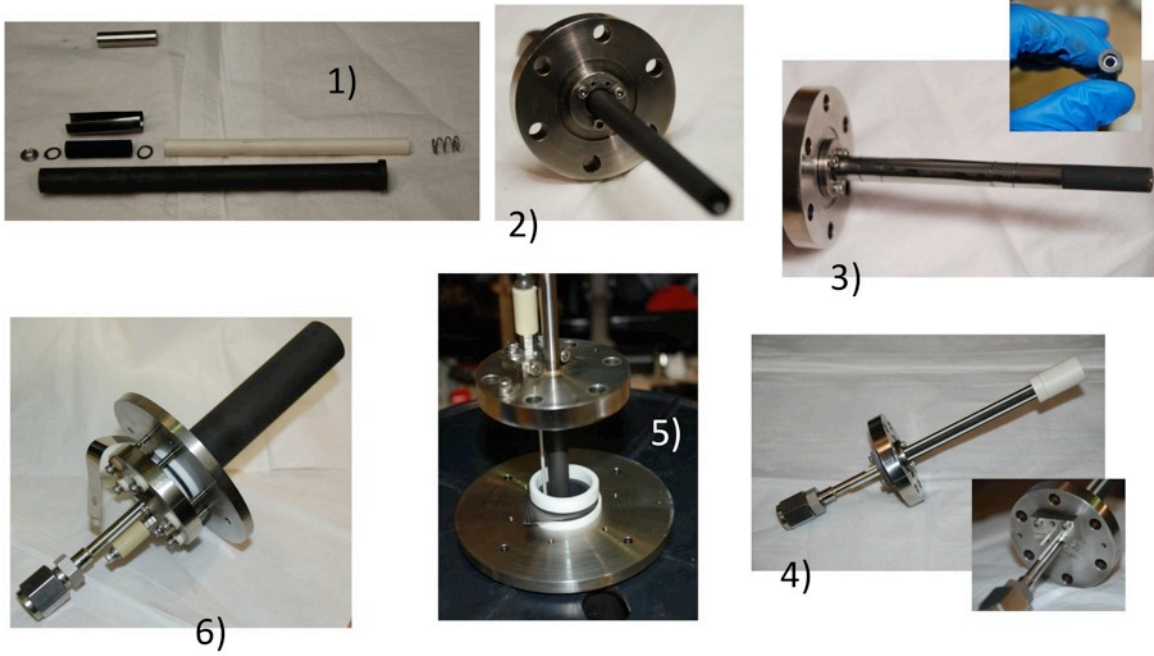
The parameters used in this equation to fit the measured EEDF are  $T_{e,fit} = 1.45$  eV and  $\Delta V = 9.4$  V. This potential shift corresponds to an energy of around 10 eV. Using  $\Delta v = \sqrt{2 q \Delta V / m}$ , this corresponds to a velocity shift of  $1.8 \times 10^6$  m/s.

## V. Conclusion

A LaB<sub>6</sub> hollow cathode with a new heater system has been constructed and successfully optimized to allow ease of operation and in-house filament replacement at a fraction of the cost as compared to previous heater designs. Next steps will involve continuing to improve upon the heater design, further characterizing the cathode's plume from Langmuir probe data, and utilizing the cathode for various electron dynamics experiments.

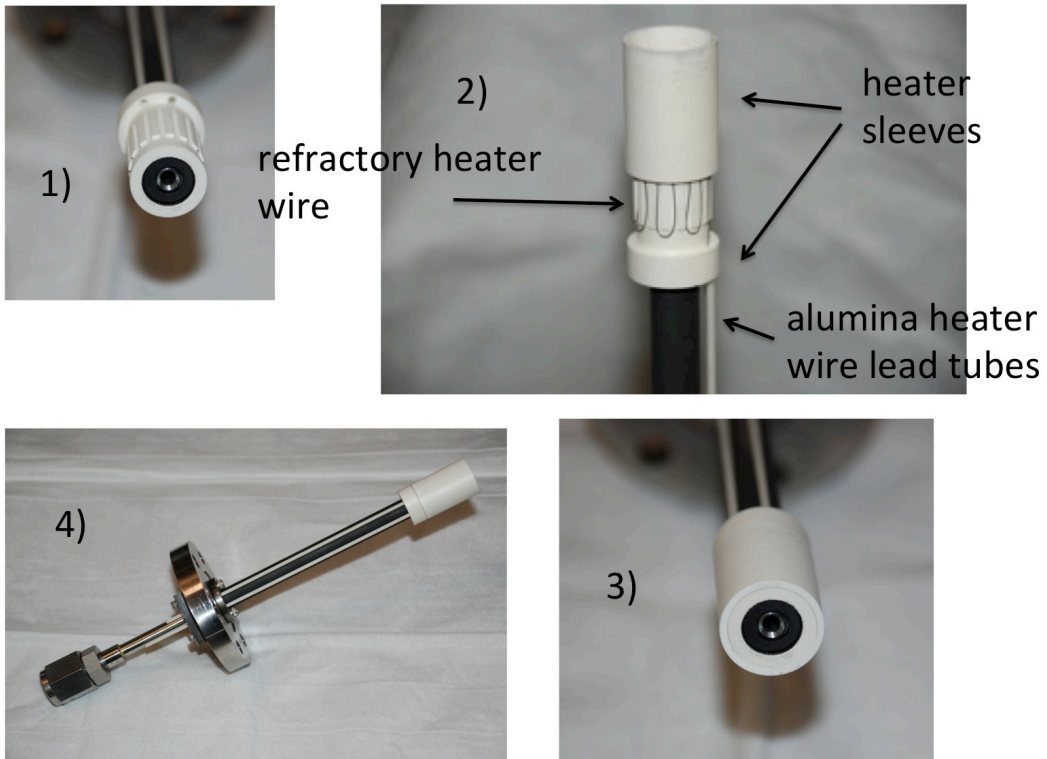
## Appendix A

### Visual Summary of the Cathode Assembly



## Appendix B

### Visual Summary of the Cathode Heater Assembly



## Acknowledgments

M. S. McDonald sends special thanks to Dan Goebel for all his invaluable assistance in the overall design of this LaB<sub>6</sub> cathode. The first author would like to thank the NASA Harriett Jenkins Predoctoral Fellowship Program (JFPF) and the Ford Foundation Predoctoral Fellowship Program for their funding support.

## References

- <sup>1</sup> Mavrodineanu, R., "Hollow Cathode Discharges - Analytical Applications," *National Institute of Standards and Technology*, vol. 89, no. 2, 1984, pp. 143–185.
- <sup>2</sup> Lafferty, J. M., "Boride Cathodes," *Journal of Applied Physics*, vol. 22, no. 3, 1951, pp. 299-309.
- <sup>3</sup> Kim, V., Popov, G., Arkhipov, B., Murashko, V., Gorshkov, O., Koroteyev, A., Garkusha, V., Semenkin, A., and Tverdokhlebov, S., "Electric Propulsion Activity in Russia," 27th International Electric Propulsion Conference, IEPC-01-05, Pasadena, CA, 2001.
- <sup>4</sup> Hofer, R. R., Goebel, D. M., and Watkins, R. M., "Compact LaB<sub>6</sub> Hollow Cathode for the H6 Hall Thruster," 54th JANNAF Propulsion Meeting, Denver, CO, 2007.
- <sup>5</sup> Goebel, D. M., Watkins, R. M., and Jameson, K. K., "LaB<sub>6</sub> Hollow Cathodes for Ion and Hall Thrusters," *Journal of Propulsion and Power*, Vol. 23, 2007, pp. 552-558.
- <sup>6</sup> Goebel, D. M., Hirooka, Y., and Sketchley, T. A., "Large-Area Lanthanum Hexaboride Electron Emitter," *Review of Scientific Instruments*, vol. 56, no. 9, 1985, pp. 1717–1722.
- <sup>7</sup> Goebel, D. M. and Watkins, R. M., "High Current Hollow Cathodes for High Power Ion and Hall Thrusters," 41st AIAA/ASME/SAE/ASEE Joint Propulsion Conference & Exhibit, AIAA 2005-4239, Tucson, AZ, 2005.
- <sup>8</sup> Goebel, D. M. and Watkins, R. M., "Compact Lanthanum Hexaboride Hollow Cathode," *Review of Scientific Instruments*, Vol. 81, No. 8, 2010, p. 083504.
- <sup>9</sup> Hofer, R. R., Katz, I., Mikellides, I. G., Goebel, D. M., Jameson, K. K., Sullivan, R. M., Johnson, L. K., AIAA-2008-4924, 44th AIAA/ASME/SAE-ASEE Joint Propulsion Conference, Hartford, CT, 2008.
- <sup>10</sup> McDonald, M. S., Gallimore A. D., Hofer R. R., and Goebel D. M., JANNAF-1192, 57th Joint Army-Navy-NASA-Air Force (JANNAF) Propulsion Meeting, Colorado Springs, CO, 2010.
- <sup>11</sup> Reid, B. M., "The Influence of Neutral Flow Rate in the Operation of Hall Thrusters," Ph.D. Dissertation, Aerospace Engineering Dept., University of Michigan, Ann Arbor, MI, 2009.
- <sup>12</sup> Lobbia, R. B., and Gallimore, A. D., "A Method of Measuring Transient Plume Properties," AIAA-2008-4650, 44th AIAA/ASME/SAE-ASEE Joint Propulsion Conference, Hartford, CT, 2008.
- <sup>13</sup> Lobbia, R. B., "A Time-Resolved Investigation of the Hall Thruster Breathing Mode," Ph.D. Dissertation, Aerospace Engineering Dept., Univ. of Michigan, Ann Arbor, MI, 2010.
- <sup>14</sup> Lieberman, M. A. and Lichtenberg, A. J., *Principles of Plasma Discharges and Materials Processing*, 2nd ed., John Wiley & Sons Inc., Hoboken, New Jersey, 2005, p. 191.
- <sup>15</sup> Shastry, R., Gallimore, A. D., and Hofer, R. R., "Near-Wall Plasma Properties and EEDF Measurements of a 6-kW Hall Thruster," 31st International Electric Propulsion Conference, IEPC-2009-133, University of Michigan, Ann Arbor, MI, 2009.